

THE GALACTIC CENTER INTERSTELLAR MEDIUM: FROM ISO TO FIRST

N.J. Rodríguez-Fernández and J.M. Martín-Pintado

Observatorio Astronómico Nacional, Instituto Geográfico Nacional, Apdo. 1143, E28800 Alcalá de Henares, Madrid, Spain

ABSTRACT

The *Infrared Space Observatory*¹ (ISO) has shown the complexity of the Galactic center (GC) Interstellar medium (ISM) detecting, not only large column densities of warm molecular gas (H₂), but the emission of neutral atoms and ions of low ionization potential (CII, OI, SiII,...) that should arise in shocked or photon-dominated regions (PDRs). In addition, ISO has also detected emission from ions like SIII, NeII, ArII, or NII (in some clouds we have even detected NeIII and OIII) that should arise from HII regions that were previously unsuspected due to the non-detection of Hydrogen recombination lines. Here we review some ISO results on the large scale study of the GC ISM and in particular, on the heating mechanisms of the clouds. Although, shocks should play an important role on the physics and chemistry of the GC ISM, ISO shows that the effect of radiation on the heating of the gas cannot be ruled out with the simple argument that the dust temperature is lower than that of the gas.

Key words: ISM: clouds, continuum, lines and bands– Galaxy: center - Infrared: ISM

1. INTRODUCTION

In the few hundred central parsecs of the Galaxy (hereafter GC) clouds are denser ($n_{\text{H}_2} \sim 10^4 \text{ cm}^{-3}$), more turbulent ($\Delta v \sim 20 \text{ Km s}^{-1}$), and hotter than the clouds of the galactic disk. There is a widespread warm gas component with temperatures of 100-200 K first known by NH₃ observations (see e.g. Hüttemeister et al. 1993) and now studied in detail with H₂ pure-rotational lines observations by ISO (Rodríguez-Fernández et al. 2001, hereafter RF01). The heating of the warm gas component over large regions where the dust temperatures are much lower than those of the gas is a puzzle. The discrepancy between the dust and the gas temperature is usually considered to imply a mechanical, rather than radiative, heating mechanism (Wilson et al. 1982, Güsten et al. 1985). With the purpose of investigating the heating mechanisms of the GC

¹ Based on observations with ISO, an ESA project with instruments funded by ESA Member States (especially the PI countries: France, Germany, the Netherlands and the United Kingdom) and with the participation of ISAS and NASA

molecular clouds, we have studied a sample of 18 clouds distributed all along the CMZ (Central Molecular Zone) at millimeter and infrared wavelengths using the ISO and the IRAM-30m telescopes.

ISO has allowed us to study the thermal balance of the GC clouds by observing the major coolants of the gas with temperatures of a few hundred Kelvin like H₂, OI, or CII. In the following we will review what we have learned from infrared (IR) and mm wavelength studies in the field of the large scale study of the GC ISM.

2. THE MOLECULAR GAS

2.1. GAS COLUMN DENSITIES FROM THE CO DATA

We have observed the J=1-0 and J=2-1 lines of C¹⁸O and ¹³CO with the IRAM-30m telescope. The J=2-1 to J=1-0 line ratios are compatible with cold (20 K) and dense gas (10^4 cm^{-3}) or warmer ($\sim 100 \text{ K}$) but less dense gas (10^3 cm^{-3}). However, the column densities derived in both cases are rather similar. In general, if one considers a mixture of cold and warm gas the total column densities traced by CO will be similar to those derived for gas at 20 K, which vary from source to source but are in the range of $\sim 1 - 6 \cdot 10^{22} \text{ cm}^{-2}$ (RF01)

2.2. WARM H₂

We have observed several H₂ pure-rotational lines (from the S(0) to S(5) lines) with the SWS spectrometer on board ISO. The S(3) line is strongly absorbed by the 9.7 μm band of the silicates and has only been detected in the sources with the most intense S(1) emission. The visual extinction derived from the H₂ data is $\sim 30 \text{ mag}$. After correcting for extinction one finds that the excitation temperature derived from the S(0) and S(1) lines (T_{32}) is between 130 and 200 K while that derived from the S(4) and S(5) lines when detected is 500-700 K. There is not a clear dependence of T_{32} on the distance to the Galactic center. Extrapolating the populations in the J=2 and J=3 levels (as derived from the S(0) and S(1) lines) to the J=0 and J=1 levels at the temperature T_{32} one finds that the total warm H₂ column density varies from source to source but is typically of $1-2 \cdot 10^{22} \text{ cm}^{-3}$. The column density of gas at $\sim 600 \text{ K}$ is less than 1% of the column density at $\sim 150 \text{ K}$. On average, the warm H₂ column

densities are about $\sim 30\%$ of the total H_2 column densities derived from CO. For a few clouds the fraction of warm gas is as high as 77% or even $\sim 100\%$. This implies that for these clouds almost all of the CO emission should arise from warm gas (see RF01). Comparing with the NH_3 observations of Hüttemeister et al. (1993) one finds relatively high NH_3 abundances of a few 10^{-7} in both the warm and the cold gas.

There are indirect arguments that points both to shocks and to photo-dissociation regions (PDRs) as the heating mechanism of the warm gas (see RF01 for a complete discussion). Direct comparison of the H_2 data with PDRs and shocks models (see Fig. 1) indicate that the S(4) and S(5) lines trace the densest gas in the GC clouds (10^6 cm^{-3}) heated in PDRs, shocks, or both. Nevertheless, to explain the large column densities of gas at $\sim 150 \text{ K}$ traced by the S(0) and S(1) lines several less dense PDRs (with $G_0 = 10^3$ and $n = 10^3 \text{ cm}^{-3}$) or low velocity shocks ($< 10 \text{ km s}^{-1}$) in the line of sight are required. The curvature of the the population diagrams is in agreement with the temperature gradient expected in a PDR (Fig. 1b) but probably also with a composition of shocks with different velocities. In summary, it is difficult to know if the H_2 emission arises in PDRs or shocked regions.

3. THE IONIZED GAS

With both the LWS and SWS spectrometers on board ISO we have detected fine structure lines of ions like [N II] $122 \mu\text{m}$, [SIII] 33 and $18 \mu\text{m}$ or [Ne II] $12 \mu\text{m}$ in most sources. We have even detected [N III] $57 \mu\text{m}$, [O III] 88 and $52 \mu\text{m}$ or [Ne III] $15.6 \mu\text{m}$ in the few sources located closer to the Galactic center. All these lines of ions with high excitational potentials must arise in H II regions. Otherwise, one needs to invoke J-shocks with velocities $\gtrsim 100 \text{ km s}^{-1}$ and there is no hint of such strong shocks from the line profiles or the radial velocities of any observed line. We derive effective temperatures for the ionizing radiation of $\sim 35000 \text{ K}$, typical of an O7 star (see Martín-Pintado et al. 1999, 2000).

We have observed the $\text{H}35\alpha$ and $\text{H}41\alpha$ recombination lines in all the sources of our sample with the IRAM-30m telescope. We have not detected any of these lines in any source (Martín-Pintado et al. 1999, 2000). Assuming line widths as large as 100 km s^{-1} and an electron temperature (T_e) of 8000 K we can set a conservative *upper limit* to the number of Lyman continuum photons emitted per second by the excitation source of $\sim 3 \cdot 10^{47} \text{ s}^{-1}$. This rate is typical of a star with a spectral type B0 or later and effective temperature $\leq 30000 \text{ K}$.

This implies that the number of Lyman continuum photons derived from the radio recombination lines is not the total number of those photons emitted by the ionizing source. The apparent inconsistency between the radio recombination lines and the fine structure lines disappears if one considers that the HII regions are more extended than

the 30-m telescope beam, e.g., that the ionizing stars are surrounded by cavities with sizes of $\sim 1 - 2 \text{ pc}$ (Martín-Pintado et al. 1999, 2000).

4. THE DUST

Figure 2 shows the dust continuum spectra toward a representative sample of sources. Any other spectrum is very similar to one of those in Fig. 2. The wavelength of the maximum of emission varies from $\sim 110 \mu\text{m}$ for M+0.76-0.05 and other sources with galactic longitude $> 1^\circ$ to $\sim 80 \mu\text{m}$ for the sources located in the Sgr C region and even to $\sim 55 \mu\text{m}$ for a few sources located close to the Radio Arc.

To explain the dust emission one needs at least two grey bodies. Figure 3 displays the dust emission of the sources with coldest (M+0.76-0.05) and warmest dust (M+0.21-0.12) together with the predictions of a model with two grey bodies at different temperatures. For the predictions we have used the following expression:

$$S_\lambda = \Omega[f_c(1-e^{-\tau_c})B(T_c, \lambda) + f_w e^{-\tau_c}(1-e^{-\tau_w})B(T_w, \lambda)] \quad (1)$$

where $B(T, \lambda)$ represents the Planck function and the opacity, τ , is given by:

$$\tau(\lambda) = 0.014A_V(30/\lambda)^\alpha \quad (2)$$

where A_V is the visual extinction in magnitudes and λ expressed in μm . This model assumes that the warmer component is being extinguished by the colder one. Taking $\Omega = 80'' \times 80''$ (the LWS beam) we obtain good fits for the values of the parameters listed Table 1. To explain

Table 1. Parameters of the grey bodies shown in Fig. 3

Source	A_v	α	T	f
M+0.76-0.05	49	1.5	16	10
	7.5	1	30	1
M+0.21-0.12	50	1.5	16	6
	2.2	1	47	1

the emission at large λ 's it is necessary a grey body with temperature $\sim 15 \text{ K}$. The visual extinction associated to this component would be 30–50 mag. To explain the large fluxes observed at large λ 's, filling factors (f) > 1 are needed. The temperature of the cold component does not vary much from source to source.

In addition to the cold dust component a warmer one is also required. This component would fill the beam and its temperature varies from source to source from the $\sim 30 \text{ K}$ of M+0.75-0.05, M+3.06+0.34 and M+1.56-0.30 (Rodríguez-Fernández et al. 2000) to the $\sim 45 \text{ K}$ of M+0.21-0.12 and M+0.35-0.06. The visual extinction associated to this component would be $\sim 2-8$ mag, that is, 5-10 % of the extinction due to the cold dust component.

Clearly, a heating mechanism is needed to raise the dust temperature from ~ 15 K to 30 K or even 45 K. For the standard dust-to-gas ratio the extinction caused by the warm dust component is equivalent to a H_2 column density of $2\text{--}8 \times 10^{21} \text{ cm}^{-2}$. These equivalent column densities are only a factor of 2 lower than the column densities of warm gas as derived from the H_2 pure-rotational lines. The simplest explanation is that both the warm gas and dust arise in low-density PDRs like those modeled by Hollenbach et al. (1991).

In the external layers of the PDR the gas is heated via photoelectric effect in the grain surfaces without heating the dust to high temperatures. For instance, in their “standard” model ($n = 10^3 \text{ cm}^{-3}$ and $G_0 = 10^3$), the gas can reach temperatures of 100–200 K in the first 3 mag of visual extinction into the cloud where on average the dust temperature would be ~ 35 K (see Fig. 3 of Hollenbach et al. 1991). Those values for the PDR parameters are quite reasonable for the GC ISM at large scale based on average densities and the far-IR continuum (see discussion in Pak et al. 1996). PDR models with $n \sim 10^3 \text{ cm}^{-3}$ and $G_0 \sim 10^3$ can also explain the H_2 excitation temperatures traced by the S(0) and S(1) lines and the large scale emission of the $\text{H}_2 v = 1 - 0$ S(1) line (Pak et al. 1996).

In this scenario, the warm dust component would be located at the GC while the cold dust emission would arise both from the GC clouds and from clouds in the line of sight (typically ~ 25 mag of visual extinction are due to material located between us and the GC region).

5. CONCLUSIONS

ISO has, for the first time, measured directly the column densities of warm molecular gas in the GC. On average, the warm H_2 represents a fraction of $\sim 30\%$ of the total H_2 column densities derived from ^{13}CO and C^{18}O observations.

ISO has also detected fine structure lines of ions with high ionization potential that should arise from HII regions. The comparison of the fine structure lines with Hydrogen recombination lines at mm wavelengths shows evidences for an extended ionized component with high effective radiation temperature.

This suggests the presence of a PDR in the interface between the HII region and the molecular material that should contribute to the heating of the warm gas and the dust component with temperatures of 30–45 K.

There are many evidences that shocks play an important role in the physics and chemistry of the GC ISM. The high abundances of molecules which are easily photodissociated like NH_3 , SiO (Martín-Pintado et al. 1997) and $\text{C}_2\text{H}_5\text{OH}$ (Martín-Pintado et al. 2001) suggest that they should be sputtered from the grains by shocks. Nevertheless, ISO points out that the effect of UV radiation on the GC ISM (and in particular on the heating of the molecular

gas) cannot be ruled out with the simple argument that the dust temperature is lower than that of the gas.

FIRST will help to understand the energetics of the GC ISM. For instance, the high spectral and spatial resolution that the HIFI instrument will achieve, will be of great interest to study the interplay between the ionized material and the warm molecular gas.

ACKNOWLEDGEMENTS

NJR-F acknowledges *Consejería de Educación Cultura de la Comunidad de Madrid* for a pre-doctoral fellowship. This work has been partially supported by the Spanish CICYT and the European Commission under grant numbers ESP-1291-E and 1FD1997-1442.

REFERENCES

- Draine B. T., Roberge W. G., Dalgarno A., 1983, ApJ 264, 485
 Fuente A., Martín-Pintado J., Rodríguez-Fernández N.J., Rodríguez-Franco A., de Vicente, P., 1999, ApJ 518, L45
 Güsten R., Walmsley C. M., Ungerechts H., Churchwell E., 1985, A&A 142, 381
 Hollenbach D. & McKee C. F., 1989, ApJ 342, 306
 Hollenbach D.J., Takahashi T., Tielens A.G.G.M., 1991, ApJ 377, 192
 Hüttemeister S., Wilson T.L., Bania T.M., Martín-Pintado J., 1993, A&A 280, 255
 Martín-Pintado J., de Vicente P., Fuente A., Planesas P., 1997, ApJ 482, L45
 Martín-Pintado J., Rodríguez-Fernández N.J., de Vicente P., Fuente A., Wilson T.L., Hüttemeister S., Kunze D., 1999, in: Cox P. & Kessler M. (eds.) *The Universe as Seen by ISO*, ESA-SP 427, 711
 Martín-Pintado J., Rodríguez-Fernández N. J., de Vicente P., Fuente A., Wilson T. L., Hüttemeister S., Kunze D., 2000, *ISO beyond the peaks*, held 2-4 February 2000, at VILSPA., ESA SP-456, in press
 Martín-Pintado J., Rizzo J.R., de Vicente P., Rodríguez-Fernández N. J., Fuente A., 2001, ApJ Letters, in press
 Pak S., Jaffe D.T., Keller L.D., 1996, ApJ 457, L43
 Rodríguez-Fernández N.J., Martín-Pintado J., de Vicente P., Fuente A., Hüttemeister S., Wilson T.L., Kunze D., 2000, A&A 356, 695
 Rodríguez-Fernández N.J., Martín-Pintado J., Fuente A., de Vicente P., Wilson T.L., Hüttemeister S., 2001, A&A 365, 174; RF01
 Wilson T.L., Ruf K., Walmsley C.M., Martin R.N., Pauls T.A., Batrla W., 1982, A&A 115, 185

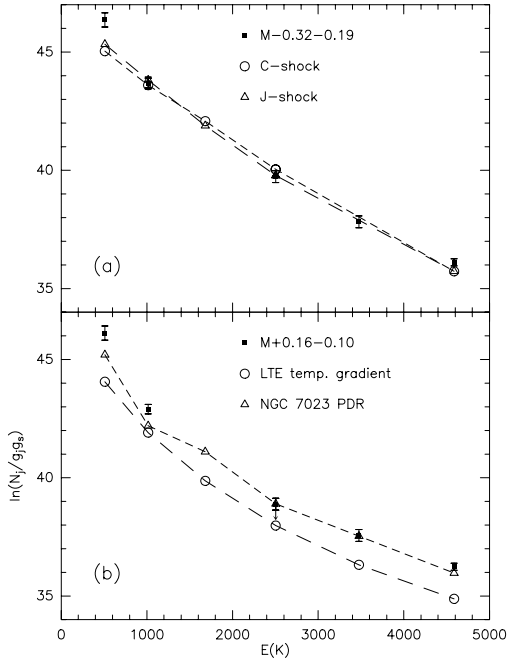


Figure 1. **a)** Population diagram for $M-0.32-0.19$ (squares) corrected for 30 mag. of visual extinction. The errorbars represent upper limits to the flux calibration uncertainties. For comparison, it also displays the population diagrams derived from the model of Draine et al. (1983) of a shock with velocity $\sim 12 \text{ km s}^{-1}$ and preshock density 10^6 cm^{-3} (circles and dashed lines). Triangles and long-dashed lines are used to plot the population diagram derived from the J-shock model of Hollenbach & McKee (1989) for a velocity of 50 km s^{-1} and a preshock density of 10^6 cm^{-3} . **b)** Comparison of the population diagram derived for $M+0.16-0.10$ (squares) with the results of Fuente et al. (1999) for the NGC 7023 PDR (triangles and dashed line) and the population diagram one obtains integrating the H_2 emission along the temperature and H_2 abundance gradient derived by Burton et al. (1990) for a PDR with density of 10^6 cm^{-3} and $G_0 = 10^4$ (open circles)

Figure 2. LWS full grating spectra toward some of the clouds. A constant has been added to some of them for display purposes

Figure 3. LWS spectra (dots) and fits to $M+0.21-0.12$ (blue) and $M+0.76-0.05$ (black). Dotted and solid lines represent a cold and a warm grey body, respectively, with parameters given in Table 1. The curves plotted with empty squares are the total emissions as defined by Eq. 1

This figure "figure2.gif" is available in "gif" format from:

<http://arxiv.org/ps/astro-ph/0101350v1>

This figure "figure3.gif" is available in "gif" format from:

<http://arxiv.org/ps/astro-ph/0101350v1>